RSC Advances

ROYAL SOCIETY OF CHEMISTRY

www.rsc.org/advances

Journal Name

ARTICLE

High temperature friction and wear properties of graphene oxide/polytetrafluoroethylene composite coatings deposited on stainless steel

Received 00th January 20xx,
Accepted 00th January 20xx

DOI: 10.1039/x0xx00000x

www.rsc.org/

N. Nemati,[a, b] M. Emamy,[a] S. Yau,[b, c] J- K. Kim,[b, c] and D- E Kim[b, c, *]

Polytetrafluoroethylene (PTFE) coating is known as a low friction material that is often used as a solid lubricant coating. However, due to its relatively weak mechanical strength, wear has been a critical issue which needs to be overcome. In the present work, a composite coating comprised of PTFE and graphene oxide (GO) was investigated with the aim to significantly improve the wear resistance of PTFE, in both room and elevated temperature conditions. PTFE/GO (PG) composite coatings with varying amounts of GO in the PTFE matrix were successfully deposited on stainless steel (SS) substrates by the spin coating method. Both micro- and macro-scale tests were performed in order to assess the tribological properties of the coatings under a wide range of normal load. Results of the micro-scale tests showed that the coefficient of friction and the wear rate could be remarkably reduced to 0.1 and 0.65×10^{-9} $mm^3/N{\cdot}m$, respectively, with inclusion of 15 vol.% of GO in the PTFE matrix. This coating also demonstrated low friction and wear properties up to 400 ^{o}C in the macro-scale tests. The superior tribological properties of the PG coating were attributed to the synergistic effects of PTFE and GO. Specifically, the existence of a rather homogeneous dispersion of high strength GO in the low friction PTFE matrix allowed for generation of a self-lubricating film along the wear track.

1. Introduction

With increasing demand for highly energy-efficient machines and environmental cleanliness, the need to improve the overall performance of mechanical components has been growing. In this regard, reduction of friction and wear to conserve energy and minimize waste products still remains as a challenge in various technological applications. Particularly in situations where liquid lubricants cannot be used due to high temperature or vacuum conditions, solid lubricants in the form of coatings need to be used to attain low friction and wear of moving mechanical components [1–4].

Numerous types of solid lubricants have been developed over the years to satisfy the operational needs of different applications. Nevertheless, solid lubricants with superior tribological and environment-friendly characteristics are continuously sought to meet the demands of emerging technologies. In line with the requirement that solid lubricants should have low shear strength, relatively soft materials, such as graphite, polyetheretherketone (PEEK), polytetrafluoro-ethylene (PTFE), and polyethylene oxide (PEO) have been utilized as low friction coating materials [5–7]. Though these materials are able to reduce friction of metallic surfaces, there is still a need to improve their wear resistant properties.

A well-adopted strategy to enhance the mechanical strength of a soft coating is to use additives [8]. For this purpose, environment-friendly lubricants that contain novel carbon-based materials are widely utilized in the development of anti-wear coatings and also as lubricant additives for various polymeric and metallic coating systems. Carbon based materials, such as single and multi-wall carbon nano-tubes (CNTs) [5,9], nano-size graphene sheets [1,10], fullerene (C60) [3] and graphene oxides (GOs) [4], can be used to enhance the wear resistant properties of various lubricants and coatings. Carbon nanotubes have been shown to be effective in reducing the wear of PTFE by Chen et al. [11]. Similarly, it has been recently shown that other carbon-based fillers, such as ultrafine diamond particles [12] and graphene platelets [13], are able to reduce the wear rate of PTFE. Among such carbon-based materials, graphene, which is a two-dimensional hexagonal arrangement of sp^2 carbon atoms, has recently attracted a great amount of interest, because of its outstanding properties. Some advantages of graphene include excellent strength, high modulus, high hardness, and anisotropic electrical and thermal properties [8,14]. Much of these attributes are beneficial for attaining superior tribological properties. As graphene is less than 1 nm in thickness, it has been largely explored for applications in micro-scale applications. For example, several studies have shown that mono-layer

[a] Center of Excellence for High Performance Materials, School of Metallurgy and Materials Engineering, College of Engineering, University of Tehran, Tehran, Iran
[b] Center for Nano-Wear, Yonsei University, Seoul 120-749, Republic of Korea
[c] Department of Mechanical Engineering, Yonsei University, Seoul 120-749, Republic of Korea
† * Corresponding author (Tel: +82221232822; E-mail: kimde@yonsei.ac.kr)

graphene coatings are favorable for in decreasing surface energy and reducing friction of silicon-based materials [10,14–16]. In another study, solution-processed graphene (SPG) was prepared by chemical exfoliation of highly oriented pyrolytic graphite (HOPG), which was utilized to reducing the coefficient of friction (COF) of stainless steel to a value as low as 0.14 [1].

The application potentials of graphene are not limited to micro- and nano-scale systems, but may be applied in macro-scale systems for corrosion protection [14,17,18]. Also, graphene has been utilized as additives in oil for improved lubricity and wear resistance [4,15,19]. In a recent study using graphene nanoplates (GNPs) as a reinforcing material in Ni_3Al matrix, it was found that the lowest COF and wear rate up to 600 ^oC under a normal load of 10 N were 0.25 and 4.1–5.3×10^{-6} mm^3/Nm, respectively [20]. Furthermore, the effects of various additives on the tribological properties of PTFE were investigated. It was found that the wear rates of the PTFE composite coatings for all the additives were in the range of ~10^{-5} mm^3/Nm [21]. Huang et al. reported that application of graphene nano-sheets as additive in paraffin oil could reduce the COF value of pure paraffin from 0.1 down to 0.02 in the liquid lubrication state [10].

Along with graphene, graphene oxide (GO) has received a great deal of attention in various mechanical and electrical applications such as super capacitors, hydrogen storage, and wear reduction [4,22], due to its superior electrical and mechanical properties [23,24]. For tribological applications, the potential of utilizing GO as a self-lubricating material has been previously investigated [8,19,25–27]. Also, studies have demonstrated the effectiveness of GO as a friction and wear reducing agent when incorporated in a polymer or a metal matrix [1,4,26,28]. According to a recent study, a mere 1 wt.% inclusion of GO and polytetrafluoroethylene (PTFE) in polyimide or epoxy resulted in a nearly 60% reduction in the friction coefficient and more than two orders of magnitude reduction in the wear rate [4]. However, the polymeric composite was in a bulk form which limited the strength and stiffness of the component.

The aim of the present study was to develop a low friction and wear composite coating based on PTFE and GO (from here on referred to as PG coating). Stainless steel (SS) was chosen as the substrate material due to its importance and wide usage in various engineering applications. In order to attain a comprehensive understanding of the scale effect on the friction and wear behaviors of the composite coating, both micro- and macro-scale tribotests were performed. Furthermore, the performance of these coatings at elevated temperatures up to 400 ^oC was assessed.

2. Materials and methods

2.1 Material preparation

In order to fabricate the PTFE/GO (PG) composite coating, GO nano-powders with an average particle size of 20 nm (UniNano Teck) were first dispersed in deionized water (DI) to acquire the desired volume fraction. Dispersion process was done by means of sonication in ambient condition for 1 h. Second, PG solutions with various volume fractions (0, 5, 10, 15 vol.%) of PTFE/GO were blended for 1 h using an ultrasonic bath followed by magnetic stirring for another 1 h in 80 ºC DI water bath to form a homogeneous dispersion of GO in the PTFE matrix. The PTFE solution composed of 90 wt.% PTFE particles (Aldrich, average M_w ~ 100,000) with a diameter of about 20 nm that were uniformly dispersed in ammonium ($NH_4(OH)$).

A commercial spin-coater (YI Engineering YS- 100) was used to deposit the PTFE and PG composite coatings on pre-cleaned SS substrates (R_a ~ 200 nm). The dynamic double-layer spin coating technique was used to deposit the coatings. Adequate amount of the solution was dropped on the substrate and rotated at 2000 RPM for 30 s. Then the solution was dropped consecutively on the substrate at an interval of ~10 s as the substrate continuously rotated at 2000 RPM for another 60 s. In order to stabilize the composite coating and increase the adhesion between the coating and the SS substrate, an annealing process was utilized. The coated specimen was annealed in a commercial hot wall furnace right after the spin coating process. The heat treatment cycle for the annealing process is shown in Fig. 1, which indicates the heating and cooling times and temperatures. By maintaining a temperature of 400 °C for 80 minutes, the PTFE and PG composite coatings were partially melted to induce the coating material to creep into the valleys of the stainless steel surface roughness. This process caused the contact area between the coating and the stainless steel substrate to be maximized, which in turn aided in enhancing the adhesive force. Specimens with different compositions were synthesized to investigate the effects of GO volume fraction on the tribological properties of the composite coatings. Bare SS and PTFE coated specimens were also prepared to use as references to be compared with the PG specimens.

2.2 Tribological testing of PTFE and PG coatings

The tribological properties of the PTFE and PG composite coatings were investigated using both micro- and macro-scale reciprocating tribotesters under ambient and elevated temperatures. For micro-scale tests, pre-cleaned 1 mm diameter SS balls with an average surface roughness of ~200 nm were used as the counter surface. All micro-tribotests were performed using a custom built system at room temperature and ~45 % relative humidity under a normal load of 50 mN and a sliding speed of 4 mm/s with a 2 mm stroke. Macro-tribotests were performed using a commercial high temperature tribotester (Neoplus Inc. RFW-160) with a 5 mm diameter SS balls with an average surface roughness of ~100 nm used as the counter surface. The tests were conducted at temperatures ranging from 25 to 400 ^oC at ~35% ambient relative humidity. Experimental conditions were set to a normal load of 5 N, a sliding speed of 4 mm/s, and a stroke of 4 mm.

During the sliding tests the friction coefficient was measured in real time through a data acquisition system. Three repeated sliding tests were carried out for each experimental condition to verify the repeatability of the results. Following the sliding

tests, the specimens were analyzed with respect to wear characteristics using surface analytical tools. Critical durability time of the coating was determined by identifying the locations where complete removal of the composite coating occurred.

2.3 Mechanical properties of specimens

The hardness and Young's modulus of the specimens were measured using a commercial nanoindenter (CSM, UNHT) equipped with a Berkovich diamond tip (R < 100 nm). The continuous depth-sensing indentation technique was used for the indentation measurements [29–31]. The indentation hardness was calculated using the Oliver-Pharr method, which was performed automatically by the software built into the equipment [29,31]. Based on the values of the Young's moduli, the maximum contact pressures were estimated using the Hertzian contact theory [30]. The mechanical properties as well as the contact pressures for the specimens are listed in Table 1. The indentation depth was maintained to be below 20% of the thickness of the coating to avoid the effect of the substrate.

2.4 Characterization of surface morphology

The surface topography and morphology of the specimens were analyzed using an atomic force microscope (AFM; Park Systems NX 10). AFM images were taken in non-contact mode at a 0.5 Hz sampling rate and a resolution of 1024 lines with 1024 pixels per line. A silicon tip with a radius of 10 nm was used as the probe. The wear track morphologies of the specimens and SS balls were observed using a scanning electron microscope (SEM; JEOL 6210) equipped with an energy dispersive X-ray spectroscopy (EDS; OXFORD INCA Energy) system. A 3D laser microscope and profiler (Keyence VK-X210) was used to measure the wear volume and thickness of the composite coatings. Raman spectroscopy (Raman; JY Horiba Labram Aramis) was employed to investigate the chemical composition of the coatings and the wear tracks. In order to assess the hydrophilic properties of the coatings, water contact angle measurements were also performed.

3. Results and discussion

3.1 Morphology and properties of coatings

Fig. 2 depicts the surface morphologies and roughness profiles of PTFE and PG coatings containing different volume percentages of GO nanoparticles after annealing, measured by AFM in non-contact mode. As can be seen, the morphologies of the coatings were relatively uniform over a scan area of about 15x15 μm^2. The average surface roughness increased with increasing GO content from 9.1 nm for 0 vol.% to 21.3 nm for 15 vol.%. Also, compared to the pure PTFE coating, it was found that the morphologies of the PG composite coatings were altered quite significantly. In the case of 5 vol.% GO coating (Fig. 2b) the initially fine fiber-like morphology of PTFE (Fig. 2a) transformed to a coarse fiber-like morphology. When the GO content increased up to 15 vol.%, the morphology of the coating transformed to a semi-honeycomb structure (Fig. 2d). The reason for the alteration in morphology with respect to GO content may be described as follows. Firstly, annealing temperature up to 400 °C caused melting of PTFE fibers but not the dispersed GO particles. Secondly, the GO dispersed in PTFE matrix served as potential sites of nucleation for recrystallization of PTFE fibers after annealing. Thus, increasing the GO content (> 5 vol.%) caused the formation of agglomerates, which reduced the potential sites of nucleation for PTFE fibers, and, finally, less oriented fiber-like morphology was formed.

In order to examine the hydrophilic properties of the coatings, contact angle measurements were carried out. Measurements were made at five different locations on the specimens and the average values were obtained. Fig. 3 shows the water contact angles for pure PTFE coating as well as PTFE/GO composite coatings. The contact angle for the pure PTFE coating was the highest at around 145^o and it gradually decreased with increasing GO content, reaching a value of 87^o for 50 vol.% GO. This trend in the contact angle variation was counter to the general knowledge that the contact angle tends to increase with increasing surface roughness in the case of hydrophobic surfaces such as PTFE. The fact that the contact angle experimental results showed an opposite trend, strongly suggested that a factor other than the surface roughness effect played a dominating role in determining the contact angle. It was proposed that the effect of the inherent hydrophilic property of GO was more profound than the surface roughness effect, thus leading to the decrease in contact angle with increasing GO content in the coating [32]. In other words, although an increase in the GO content was accompanied by increasing surface roughness of the coatings (Fig. 3), it was presumed that the surfaces were still extremely smooth (< 25 nm) which did not cause a significant variation in the contact angle. Nevertheless, even with as much as 50 vol.% of GO, the composite coating was determined to be almost hydrophobic.

Thickness of the coatings was measured using a 3D laser microscope. Fig. 4 shows the 3D laser microscope image of the PG specimen with 15 vol.% of GO and the 2D profile of the scan line indicating the thickness of the coating. The profile was taken across the scratched region, which was intentionally created to expose the substrate surface. The thickness of the coatings after annealing was measured to be 400-600 nm. This variation in coating thickness was not dependent on the vol.% of GO but rather on the variation in the fabrication process. It was expected that the variation in the coating thickness between specimens would be sufficiently reflected in the deviation in the friction and wear data of three repeated experiments.

Considering the thickness of the coating, the indentation depth for hardness measurement was kept below 120 nm to avoid the substrate effect. According to the hardness values shown in Table 1, the hardness increased with increasing GO. As expected, GO nanoparticles dispersed in the soft PTFE matrix, improved the stiffness and hardness of the coating.

3.2 Friction and wear behaviors

To assess the effects of GO content in PTFE on the friction and wear behavior of the composite coatings deposited on SS, both micro- and macro-scale tribotests were performed. In the case of the micro-scale tests, relatively low normal of 50 mN was used under ambient temperature and humidity conditions. In the case of the macro-scale tests, a relatively high normal load of 5 N was applied. Tests were performed under room temperature as well as elevated temperatures of 250 and 400 °C.

3.2.1 Micro-scale friction and wear behaviours of the PTFE and PG coatings.

Fig. 5 presents the coefficient of friction (COF) with respect to sliding cycles for bare SS and various coating specimens under 50 mN normal load for up to 10,000 cycles. As can be seen, the COF value for the bare SS was initially low and then increased rapidly to a steady state value of ~1.2. This increasing trend of COF was similar to the typical frictional behavior of other metallic materials. As sliding proceeded, wear particles were created as the surface contaminants and natural oxide layer were removed. The wear particles caused an increase in three body abrasive interaction at the sliding interface, which ultimately led to the increase in COF [32,33].

The COF values for the coated specimens were significantly lower than that of the bare SS. Furthermore, the COF was quite stable throughout the entire sliding cycles for all the coated specimens. The low and stable behavior of COF was considered to be due to the synergistic lubrication effects of PTFE and GO flakes [4,34]. As can be seen from Fig. 5, addition of GO in PTFE was effective in lowering the COF from 0.16, for pure PTFE coating, down to a value as low as 0.045, for the PG specimen with 15 vol.% GO. This observation suggested that GO flakes aided not only in strengthening the PTFE, but also in allowing easy shearing of the flakes to serve as solid lubricant particles.

The wear tracks of the specimens were analyzed after the sliding tests using a 3D laser microscope in order to assess the degree of wear. Fig. 6 shows the typical profiles of the wear tracks formed on the specimen surfaces after 10,000 cycles of the sliding. It can be seen that a distinct wear track was formed on the bare SS specimen (Fig. 6a) with a large burr formed along the side of the wear track. In the case of the PTFE coated specimen (Fig. 6b), the wear area was more than 7 times smaller than that of the bare SS. However, a significant amount of wear debris was found along the side of the wear track. For the PG (15 vol.% GO) specimen (Fig. 6c), the wear area was dramatically reduced and was measured to be more than 21 times smaller than that of the bare SS. It should be noted that even though the wear depth of the PG coating specimen was less than 1 □m, it seemed to be greater than the thickness of the coating which was in the range of 400-600 nm. Nevertheless, the fact that wears was significantly less than that of the pure PTFE coating suggested that some of the coating material still remained on the wear track to function as a protective layer. Thus, the overall results indicated that the PG composite coating was effective in significantly reducing the wear of SS.

The damage incurred by the SS ball was evaluated obtaining the 3D confocal laser microscope images of the SS ball before and after the sliding test (Fig. 7). It was found that the wear of SS ball was not significant. The only damage that could be found on the ball surface was the slight scratch mark indicated by the ellipse shown in Fig. 7b. Also, there was no evidence of material transfer to the ball. This was understandable since the coating material inherently had a low adhesion property. Thus, the wear debris originated from the wear track were just swept away and piled up at the edges of the wear track rather than stick to the counter surface or the ball.

In order to assess the quantitative wear behavior of the specimens, the wear rates were obtained using the following equation (Q1).

$$Wear\ rate\ \left(\frac{mm^3}{Nm}\right) = \frac{Wear\ volume\ (mm^3)}{normal\ load\ (N) \times Sliding\ distance\ \left(No.cycles \times Stroke\ (m)\right)} \quad (Q1)$$

The wear rates were calculated at the end of 10,000 cycles using the total wear volume. The wear volume was measured using a 3D laser microscope and a surface profiler. Fig. 8 reveals that the wear rate of the bare SS specimen was the highest, which was expected. Pure PTFE coating was effective in lowering the wear rate of the bare SS by an order of magnitude, down to 5.6×10-8 mm3/N·m. Also, incorporation of the GO nanoparticles could further reduce the wear rate of the pure PTFE coating. Extremely low wear rates in the range of 1.9×10-9 ~ 2.1×10-8 mm3/N·m could be achieved with the PG coated specimens. This range of wear rate was significantly lower than the wear rates of 10-6 ~ 10-7 mm3/N·m that were reported in previous studies using solution-processed graphene (SPG) coated on SS surface or PTFE/GO incorporated in polymer matrices [1,4].

The PG coated (15 vol.% GO) specimen showed the lowest wear rate of 1.9×10-9 mm3/N·m over 10,000 cycles. The durability of this coating was verified by performing prolonged sliding tests for 50,000 cycles. The tests were conducted five times under the same conditions to assure repeatability. Fig. 9 shows the typical wear track profile and COF results obtained from the durability test. As can be seen from Fig. 9c, the worn area measured using the 3D confocal microscope was ~ 32 μm2. This corresponded to a wear rate of 0.65×10-9 mm3/N·m which was even lower than that obtained for the test performed for 10,000 cycles. The lower wear rate obtained for the prolonged sliding test was presumably related to the running-in effect of the fresh specimen at the initial stage of sliding, during which the wear rate tends to be relatively high. Based on these test results, the extremely high wear resistant property of the PG coating with 15 vol.% GO was verified.

3.2.2 Macro-scale friction and wear behaviors of the PTFE and PG coatings.

Macro-scale tribotests were performed using the coated specimens in order to assess their friction and wear behaviors

under higher normal loads. Fig. 10 shows the COFs for various specimens with respect to number of sliding cycles for tests conducted under 5 N normal load at ambient and elevated temperatures. In the case of the ambient temperature tests, all the specimens showed a low COF of below 0.1 at the initial stage of sliding. However, COF of the pure PTFE coating increased gradually until a sudden increase in the value occurred at around 625 cycles. The drastic increase in the COF was attributed to failure of the PTFE coating. In contrast to the pure PTFE coating, the PG coating specimens maintained a low COF throughout the test duration of 1000 cycles (Fig. 10a). The COF values for the 10 vol.% and 15 vol.% GO specimens were quite similar. Thus, it was determined that incorporation of GO resulted in significant improvement of the frictional behaviour of the PTFE coating even under macro-scale testing conditions.

In the case of elevated temperature tests up to 400°C, for the pure PTFE coating at 250°C, the COF increased gradually from about 0.1 to 0.22 until ~625 cycles at which point the COF increased suddenly to about 0.4. On the other hand, the COF for the 15 vol.% GO specimen was significantly lower. For the for the 15 vol.% GO coating at 250°C, the initial COF was as low as 0.025 and maintained a low value below 0.05 up to ~ 400 cycles (Fig. 10b, c). Beyond that, the COF increased slightly to a value of about 0.12 at 1000 cycles. As for the frictional behaviour of the coatings at 400°C, it was interesting to note that for all tested specimens, low and steady COF below 0.05 could be achieved at 400°C during the initial stage of sliding. For the 15 vol.% GO specimen, the COF was as low as 0.025 at the initial stage of sliding. Beyond that, the COF increased slightly to a value of about 0.1 at 1000 cycles.

The frictional behavior of pure PTFE coating specimen with respect to temperature may be explained based on its melting temperature, which is known to be ~330°C (T_m), as well as its unique physical properties. For temperatures below T_m (i.e., for room and 250°C temperatures) the solid semi-crystalline structure of PTFE allowed for low friction, because of its viscoelastic response to the application of shear through the lamellar transfer layer mechanism [35]. More specifically, the increased chain mobility of PTFE at higher temperatures facilitated its capacity to align along the sliding direction [36,37]. For a temperature higher than T_m, the COF of PTFE with a value of 0.05 at the initial stage of sliding up to ~350 cycles, was lower than the COF at 250°C [37]. This outcome was attributed to partial melting of the PTFE. However, beyond this stage, the COF increased sharply to 0.9, which could be explained by complete failure or depletion of the PTFE coating at the sliding interface.

In the case of the PG (PTFE+15 vol.% GO) coating specimen at high temperatures, the low frictional behavior may be attributed to the synergistic effects of the solid lubrication properties of PTFE and enhanced mechanical strength of the coating due to incorporation of GO. Essentially, the solid lubrication effect could be prolonged for much longer sliding cycles due to enhanced mechanical strength, which was found to be effective even at a temperature that is above T_m. It should also be noted that unlike the case of the pure PTFE coating specimen, the PG coatings did not show any sign of drastic increase in the COF. This suggested that the PG coatings did not fail completely during the sliding tests even at elevated temperatures as the pure PTFE coating did. The gradual increase in the COF of the PG coating specimen that occurred between ~350-500 cycles for the 400°C test suggested that the state of the coating was altered during this period (Fig. 10b). However, the COF was still relatively low and it decreased again to a value below 0.1. These results suggested that the PG composite coating could maintain its relatively low frictional behavior despite alteration in the physical state of the coating.

Following the friction tests, the wear characteristics of the coatings were investigated using SEM and Raman analyses. Fig. 11 shows the SEM images of wear tracks of various specimens after 1000 sliding cycles under 5 N normal load at ambient temperature. The width of the wear track is indicative of the degree of wear. It could be found that the wear of bare SS specimen (Fig. 11a) was the highest, followed by the pure PTFE coating specimen (Fig. 11b). In the case of GO incorporated coatings, the wear track width decreased with increasing GO content. Thus, it was clearly apparent that GO significantly enhanced the wear resistance of the PTFE coating. However, it should be noted that the depth of the wear track was greater than the coating thickness as was the case observed with the PG composite coating in the micro-scale test.

As for the morphology of the wear track, evidence of abrasive, as well as adhesive wear, mechanisms was apparent on the wear track of the bare SS specimen. As for the coated specimens, the wear track morphology was relatively smooth with evidence of grooves along the sliding direction. Corresponding Raman spectroscopy data of the wear tracks are presented as inset of each SEM image in Fig. 11b-e. It should be noted that D and G peaks (i_D and i_G) of PTFE and GO appear at 1327 and 1615 cm^{-1}, respectively. From the inset figures, it could be determined that as the GO content in PTFE increased, the intensity of the D band (i_D) increased, as well. It was apparent that as wear progressed, the GO on the wear track was significantly modified due to generation of defects and disordered microstructure. This was evident from the significant reduction of the G peak intensity (i_G) in the wear track, whereas the G peak intensity was relatively high at the wear track boundary as shown in the inset figure of Fig. 11e. From the Raman analysis, it was evident that some amount of GO and PTFE remained on the wear track despite the fact that the wear depth was greater than the coating thickness. Furthermore, the characteristic of the GO was altered from its original state as noted by the change in the G peak intensity of the Raman data. Previous work have shown that formation of tribo-layers on the wear track may occur in tribological systems that utilize composite coatings containing hard particles [38]. These layers that are sometimes described as mechanically mixed layers, may form on the wear track even if the coating wears out [39]. Thus, the tribo-layer formed on the wear track that contained some GO and PTFE materials was thought to be responsible for the relatively low friction and wear behavior of the PG composite coatings.

In order to quantify the degree of wear at the macro-scale, wear rates of the specimens were obtained for the tests performed at different temperatures. Fig. 12 shows the wear rates of the bare SS specimen and various coated specimens after 1000 cycles of sliding under 5 N normal load and a temperature of 400°C. This test case was selected since it represented a severe sliding situation in which both the contact pressure, as well as the temperature, was high. Thus, the overall wear rates shown in Fig. 11 are significantly higher than those obtained from room temperature micro-scale tests shown in Fig. 8. Nevertheless, even under macro-scale high temperature conditions, the coated specimens showed 1 or 2 orders of magnitude less wear than the bare SS specimen. Also, the wear rate decreased with increasing GO content, with 15 vol.% GO resulting in the lowest wear rate of 2×10^{-7} $mm^3/N\cdot m$. It was postulated that at 400 °C the synergistic effects of partial melting of PTFE and the formation of disordered GO on the wear track resulted in the formation of a solid lubricant layer that provided low interfacial shear and good surface protection.

3.2.3 Assessment of tribological performance of the PG composite coatings.

Overall, the PG composite coatings showed low friction and wear properties under both micro- and macro-scale test conditions. As noted in Table 1, for the macro-scale tribotests conducted under 5 N normal load, the Hertzian contact pressure varied between 462-1148 MPa and for the micro-scale tribotests conducted under 50 mN normal load, it varied between 86-247 MPa depending on the GO content in the coatings. Although the contact pressure was about five times greater in the macro-scale tests, the COFs of the PG coatings were similar to those observed in the micro-scale tests. A more profound difference between the two scales was found in the wear rates of the PG coatings. The high contact pressures experienced by the coatings in the macro-scale tests resulted in higher wear rates than the micro-scale tests. This outcome was postulated to be due to the fact that under a high contact pressure, the coating essentially experienced greater amount of permanent deformation which led to a higher wear rate compared with the case of a relatively low contact pressure. Nevertheless, the wear rates of the PG composite coatings with optimum amount of GO nanoparticles in both micro- and macro-scale test conditions were relatively low. This is evident from Table 2 that shows the friction and wear properties of various carbon-based coating materials. The achievement of low wear for the PG composite coating accompanied with significant reduction in friction over a wide range of contact pressure was unique for high temperature wear resistance of solid lubricants considering other coating systems proposed in previous work [1,4,36,37].

4. Conclusions

In this work the tribological properties of a composite coating comprised of PTFE and GO were evaluated under various conditions. Both micro- and macro-scale tests were performed in order to assess the tribological properties of the coatings under a wide range of normal load and temperature. Based on the experimental results, the following conclusions may be drawn.

1. In the case of the micro-scale test condition in which the normal load was 50 mN, the wear rate of pure PTFE could be drastically reduced from 5.6×10^{-8} to 1.9×10^{-9} $mm^3/N\cdot m$ by incorporating 15 vol.% of GO in the coating. The COF was also reduced significantly from 0.16 to 0.045.
2. The low friction and wear properties of the PTFE/GO composite coatings were also confirmed in the macro-scale tests in which the normal load was 5 N. However, though the friction coefficient was quite similar for both micro and macro-scales, the wear rate was found to be higher at the macro-scale.
3. Even at an elevated temperature of 400°C, the wear rate of pure PTFE could be reduced by an order of magnitude by incorporating 15 vol.% of GO in the coating. The COF at this temperature was as low as 0.025.
4. The superior tribological properties of the PTFE/GO composite coating was attributed to the rather homogeneous dispersion of high strength GO in the low friction PTFE matrix that allowed for generation of a self-lubricating film along the wear track.
5. Analysis of the experimental results showed that PTFE/GO composite coating has a great potential to be used as a solid lubricant over a wide range of load and temperature.

Acknowledgements

This work was supported by the National Research Foundation of Korea (NRF) grant funded by the Korea government (MSIP) (No. 2010-0018289). The authors would like to thank Dr. O. Penkov for performing the hardness measurements.

References

1 D. Berman, A. Erdemir and A. V. Sumant, *Carbon N. Y.*, 2013, **54**, 454–459.

2 S. S. Kandanur, M. A. Rafiee, F. Yavari, M. Schrameyer, Z.-Z. Yu, T. a. Blanchet and N. Koratkar, *Carbon N. Y.*, 2012, **50**, 3178–3183.

3 J. Pu, Y. Mo, S. Wan and L. Wang, *Chem. Commun. (Camb).*, 2014, **50**, 469–71.

4 T. Huang, T. Li, Y. Xin, B. Jin, Z. Chen, C. Su, H. Chen and S. Nutt, *RSC Adv.*, 2014, **4**, 19814.

5 B.-H. Ryu, A. J. Barthel, H.-J. Kim, H.-D. Lee, O. V. Penkov, S. H. Kim and D.-E. Kim, *Compos. Sci. Technol.*, 2014, **101**, 102–109.

6 P. Samyn and G. Schoukens, *Polym. Compos.*, 2009, **30**, 1631–1646.

7 A. Uvarov, K. Uemura, S. Alexandrov, H. Murayama and R. Soba, pp. 500–503.

8 A. Journal, Y. Tong, S. Bohm and M. Song, 2013, **1**, 1–16.

9 X. Zhang, B. Luster, A. Church, C. Muratore, A. a Voevodin, P. Kohli, S. Aouadi and S. Talapatra, *ACS Appl. Mater. Interfaces*, 2009, **1**, 735–9.

10 H. D. Huang, J. P. Tu, L. P. Gan and C. Z. Li, *Wear*, 2006, **261**, 140–144.

11 W. X. Chen, F. Li, G. Han, J. B. Xia, L. Y. Wang, J. P. Tu and Z. D. Xu, *Tribol. Lett.*, 2003, **15**, 275–278.

12 S. Q. Lai, L. Yue, T. S. Li and Z. M. Hu, *Wear*, 2006, **260**, 462–468.

13 S. Bhargava, N. Koratkar and T. a. Blanchet, *Tribol. Lett.*, 2015, **59**.

14 O. Penkov, H.-J. Kim, H.-J. Kim and D.-E. Kim, *Int. J. Precis. Eng. Manuf.*, 2014, **15**, 577–585.

15 A. Mohamed Mahmoud Ibrahim, X. Shi, W. Zhai, J. Yao, Z. Xu, L. Cheng, Q. Zhu, Y. Xiao, Q. Zhang and Z. Wang, *Tribol. Trans.*, 2014, **57**, 1044–1050.

16 M. Liang and L. Zhi, *J. Mater. Chem.*, 2009, **19**, 5871.

17 S. Chen, L. Brown, M. Levendorf, W. Cai, S.-Y. Ju, J. Edgeworth, X. Li, C. W. Magnuson, A. Velamakanni, R. D. Piner, J. Kang, J. Park and R. S. Ruoff, *ACS Nano*, 2011, **5**, 1321–7.

18 J. S. Bunch, S. S. Verbridge, J. S. Alden, A. M. Van Der Zande, J. M. Parpia, H. G. Craighead and P. L. McEuen, *Nano Lett.*, 2008, **8**, 2458–2462.

19 J. Lin, L. Wang and G. Chen, *Tribol. Lett.*, 2011, **41**, 209–215.

20 W. Zhai, X. Shi, M. Wang, Z. Xu, J. Yao, S. Song and Y. Wang, *Wear*, 2014, **310**, 33–40.

21 Y. Sujuan and Z. Xingrong, *Tribol. Trans.*, 2014, **57**, 382–386.

22 M. Sevilla and R. Mokaya, *Energy Environ. Sci.*, 2014, **7**, 1250–1280.

23 D. A Dikin, S. Stankovich, E. J. Zimney, R. D. Piner, G. H. B. Dommett, G. Evmenenko, S. T. Nguyen and R. S. Ruoff, *Nature*, 2007, **448**, 457–460.

24 Y. Zhu, S. Murali, W. Cai, X. Li, J. W. Suk, J. R. Potts and R. S. Ruoff, *Adv. Mater.*, 2010, **22**, 3906–3924.

25 X. Shi, J. Yao, Z. Xu, W. Zhai, S. Song, M. Wang and Q. Zhang, *Mater. Des.*, 2014, **53**, 620–633.

26 H.-J. Song, X.-H. Jia, N. Li, X.-F. Yang and H. Tang, *J. Mater. Chem.*, 2012, **22**, 895.

27 E. Thangavel, S. Ramasundaram, S. Pitchaimuthu, S. W. Hong, S. Y. Lee, S.-S. Yoo, D.-E. Kim, E. Ito and Y. S. Kang, *Compos. Sci. Technol.*, 2014, **90**, 187–192.

28 J. Ou, J. Wang, S. Liu, B. Mu, J. Ren, H. Wang and S. Yang, *Langmuir*, 2010, **26**, 15830–15836.

29 C. Oliver and M. Pharr, *J. Mater. Res.*, 1992, **7**, 1564–1583.

30 O. V Penkov, V. E. Pukha, A. Y. Devizenko, H.-J. Kim and D.-E. Kim, *Nano Lett.*, 2014, **14**, 2536–40.

31 C. Oliver and M. Pharr, *J. Mater. Res.*, 2009, **19**, 3–20.

32 O. V Penkov, D. Lee, H. Kim and D. Kim, *Compos. Sci. Technol.*, 2013, **77**, 60–66.

33 M. Won, O. V Penkov and D. Kim, 2012, **4**, 1–10.

34 J. Ou, Y. Wang, J. Wang, S. Liu, Z. Li and S. Yang, *J. Phys. Chem. C*, 2011, **115**, 10080–10086.

35 N. M. Barkoula, B. Alcock, N. O. Cabrera and T. Peijs, *Polym. Polym. Compos.*, 2008, **16**, 101–113.

36 B. A. Krick, J. J. Ewin and E. J. McCumiskey, *Tribol. Trans.*, 2014, 2014, **57**, 1058-65.

37 T. Li, J. Tian, T. Huang, Z. Huang, H. Wang, R. Lu and P. Cong, *J. Macromol. Sci. Part B*, 2011, **50**, 860–870.

38 R. N. Rao, S. Das, D. P. Mondal and G. Dixit, *Wear*, 2009, **267**, 1688–1695.

39 E. Mohammad Sharifi, F. Karimzadeh and M. H. Enayati, *Mater. Des.*, 2011, **32**, 3263–3271.

Fig. 1 Heat treatment cycle applied for annealing the coatings deposited on SS substrates.

Journal Name

ARTICLE

Fig. 2 Non-contact mode AFM images of surface morphology and roughness profile of (a) PTFE, (b) PG (PTFE+5 vol.% GO), (c) PG (PTFE+10 vol.% GO) and (d) PG (PTFE+15 vol.% GO) composite coatings.

Journal Name

ARTICLE

Fig. 3 Contact angle measurement with respect to composition of coatings.

Fig. 4 (a) 3D laser microscope image of the PG (PTFE+15 vol.% GO) coating with a scratch inscribed to expose the substrate and (b) 2D profile of the scan line shown in (a) with indication of the coating thickness value.

Fig. 5 Coefficient of friction for various specimens with respect to number of sliding cycles under 50 mN normal load and ambient temperature.

Journal Name

ARTICLE

Fig. 6 Laser microscope image, 3D image, and 2D profile of the wear track formed on the specimen surface after 10,000 cycles of sliding under 50 mN normal load and ambient temperature for (a) bare SS, (b) PTFE coated SS, and (c) PG (PTFE+15 vol.% GO) coated SS specimens.

Journal Name

ARTICLE

Fig. 7 Laser microscope image of 1 mm SS ball (a) before and (b) after 10,000 cycles of sliding against PG (PTFE+15 vol.% GO) coated SS specimen under 50 mN normal load and ambient temperature. The ellipse in (b) indicates the surface damage incurred by the ball during the sliding test.

Fig. 8 Wear rate values of bare SS specimen and various coated specimens after 10,000 cycles of sliding under 50 mN normal load and ambient temperature.

Journal Name

ARTICLE

Fig. 9 (a) Laser microscope image, (b) 3D image, (c) 2D profile of the wear track and (d) coefficient of friction with respect to number of sliding cycles for the PG (PTFE+15 vol.% GO) coated SS specimen. Durability test condition was 50,000 cycles of sliding under 50 mN normal load and ambient temperature.

Fig. 10 Coefficient of friction for various specimens with respect to number of sliding cycles under 5 N normal load at (a) ambient temperature, (b) elevated temperatures and (c) magnified inset for better resolution of first 400 cycles of elevated temperature COF data.

Fig. 11 SEM images and Raman analyses of the wear tracks after 1000 sliding cycles under 5 N normal load at ambient temperature: (a) Bare SS, (b) PTFE coated SS, (c) PG (PTFE+5 vol.% GO) coated SS, (d) PG (PTFE+10 vol.% GO) coated SS, and (e) PG (PTFE+15 vol.% GO) coated SS.

Fig. 12 Wear rate values of bare SS specimen and various coated specimens after 1000 cycles of sliding under 5 N normal load and temperature of 400^{o}C.

Journal Name

ARTICLE

Table 1. Nanohardness, Young's modulus and maximum Hertzian contact pressure values for PTFE and PTFE/GO composite coatings.

Specimen	Nanohardness (MPa)	Young's Modulus (GPa)	Hertzian contact pressure (MPa) at 50 mN normal load	Hertzian contact pressure (MPa) at 5 N normal load
PTFE coated SS	4.5±0.8	3.6±0.45	~ 86.6	~ 465
PG (PTFE+5 vol.% GO) coated SS	6.9±1.24	6.55±0.91	~ 127.8	~ 593.2
PG (PTFE+10 vol.% GO) coated SS	7.2±2.12	5.6±3.21	~ 115.5	~ 536
PG (PTFE+15 vol.% GO) coated SS	10.1±1.53	13.7±6.91	~ 204.3	~ 984.1
PG (PTFE+50 vol.% GO) coated SS	32.1±1.61	18.7±5.94	~ 247.4	~ 1148.5

Table 2. Comparison of friction and wear behaviors of selected carbon-based materials and coatings.

Materials	Tribotest configuration and load	Remarks
Solution-processed graphene coated on SS [1]	Room temperature; ball-on-disk tribotest; 2 N applied load	Minimum wear rate ~0.03×10^{-7} mm3/Nm Minimum COF ~ 0.15
Graphene–C60 hybrid films - coated on silicon [3]	Room temperature; reciprocating tribotest; 0-150 nN applied load	Minimum wear rate (not reported) Minimum COF ~ 0.25
Graphene oxide/nano- polytetrafluoroethylene hybrid added in polyimide and epoxy matrices (bulk material) [4]	Room temperature; reciprocating tribotest; 6-12 N applied load	Minimum wear volume ~10^{-2} μm^3 Minimum COF ~ 0.3 (for the 33/67 wt.% of CNT/PEO ratio)
Carbon nanotube–polyethylene oxide composite coated on silicon [5]	Room temperature; reciprocating tribotest; 10 mN applied load	Minimum wear rate ~10^{-6} mm^3/Nm Minimum COF ~ 0.17
Carbon-nanotube-filled PTFE composite (bulk material) [11]	Room temperature; block-on-steel ring tribotest; 200 N applied load	Minimum wear rate ~ $1x10^{-5}$ mm^3/Nm Minimum COF ~ 0.4
NiAl–1.5 wt% graphene composite (bulk material) [15]	Room temperature; pin-on-disk tribotest; 12 N applied load	Minimum wear rate ~ $1x10^{-5}$ mm^3/Nm Minimum COF ~ 0.4
PTFE; PTFE + bronze; PTFE + carbon (23%) + graphite (2%); PTFE + glass fiber; PTFE + carbon fiber; PTFE + polyphenyl (bulk material) [21]	Temperature range of RT-180 °C; block-on-steel ring tribotest; 200 N applied load	For room temperature: Minimum wear rate ~3.6×10^{-5} mm^3/Nm Minimum COF ~ 0.15 For 180 °C: Minimum wear rate ~19×10^{-5} mm^3/Nm Minimum COF ~ 0.16
Graphene oxide/ polytetrafluoroethylene composite coated on stainless steel [present work]	Temperature range of RT- 400 °C; reciprocating tribotest; 50mN and 5 N applied load	For room temperature and 50 mN applied load: Minimum wear rate ~1.9×10^{-9} mm^3/Nm Minimum COF ~ 0.045 For 400 °C and 5 N applied load: Minimum wear rate ~2×10^{-7} mm^3/Nm Minimum COF ~ 0.025

Journal Name

ARTICLE

Figures and captions

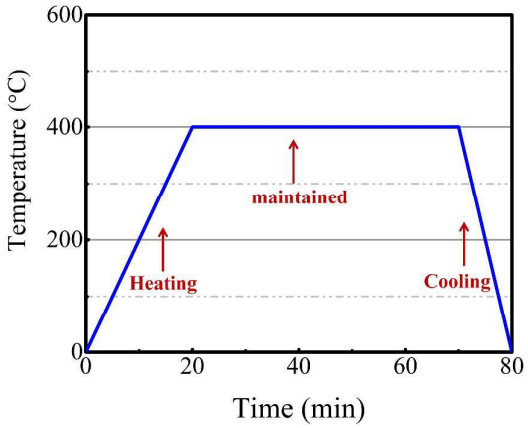

Fig. 1 Heat treatment cycle applied for annealing the coatings deposited on SS substrates.

Journal Name

ARTICLE

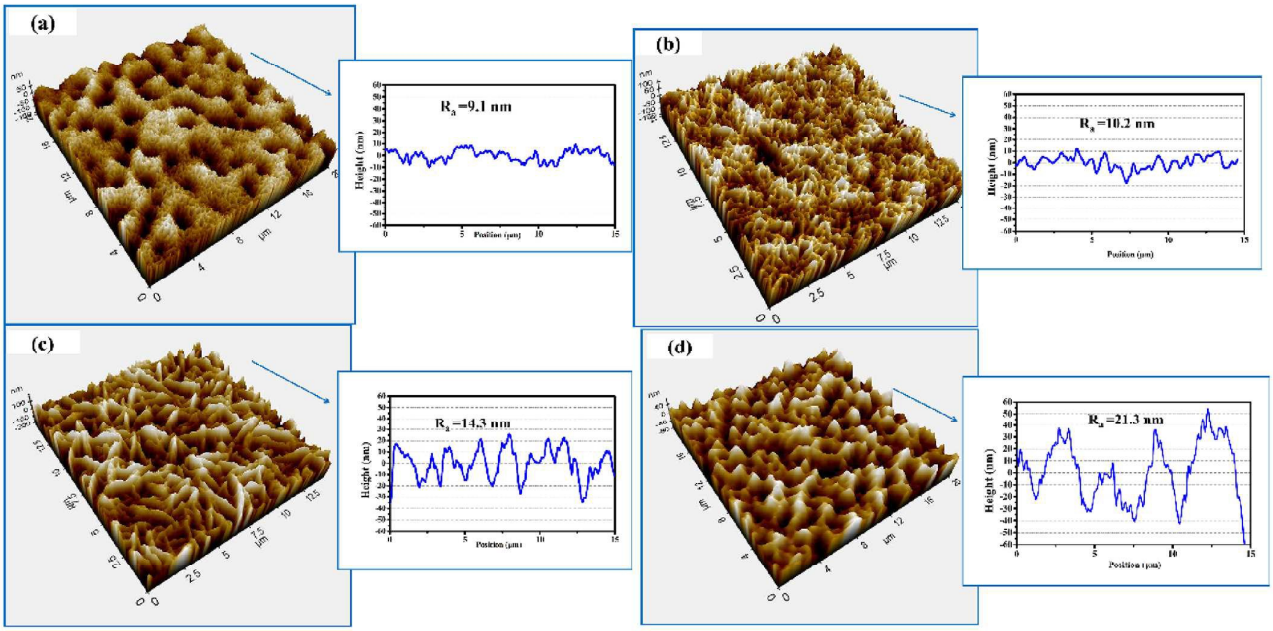

Fig. 2 Non-contact mode AFM images of surface morphology and roughness profile of (a) PTFE, (b) PG (PTFE+5 vol.% GO), (c) PG (PTFE+10 vol.% GO) and (d) PG (PTFE+15 vol.% GO) composite coatings.

Journal Name

ARTICLE

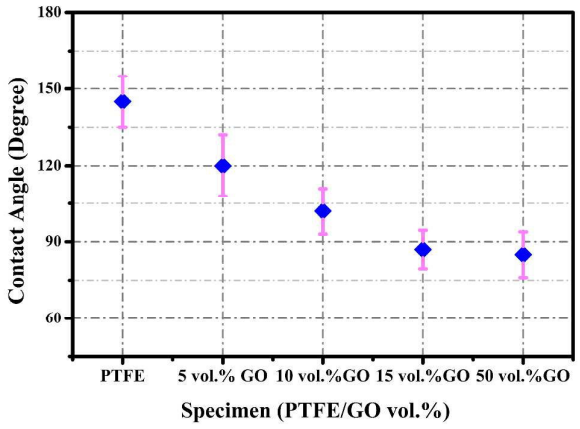

Fig. 3 Contact angle measurement with respect to composition of coatings.

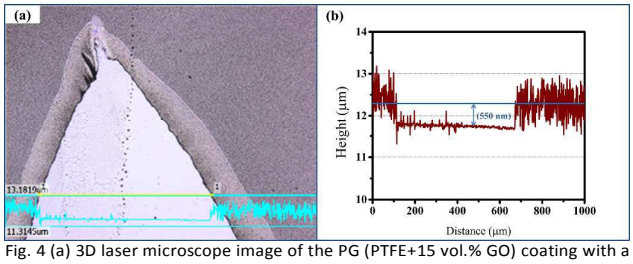

Fig. 4 (a) 3D laser microscope image of the PG (PTFE+15 vol.% GO) coating with a scratch inscribed to expose the substrate and (b) 2D profile of the scan line shown in (a) with indication of the coating thickness value.

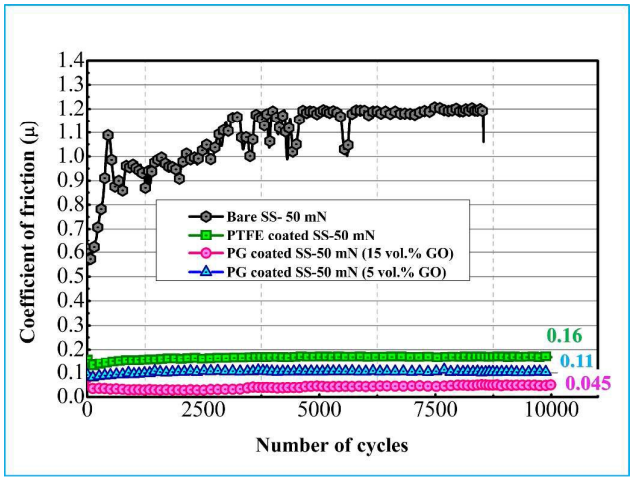

Fig. 5 Coefficient of friction for various specimens with respect to number of sliding cycles under 50 mN normal load and ambient temperature.

Journal Name

ARTICLE

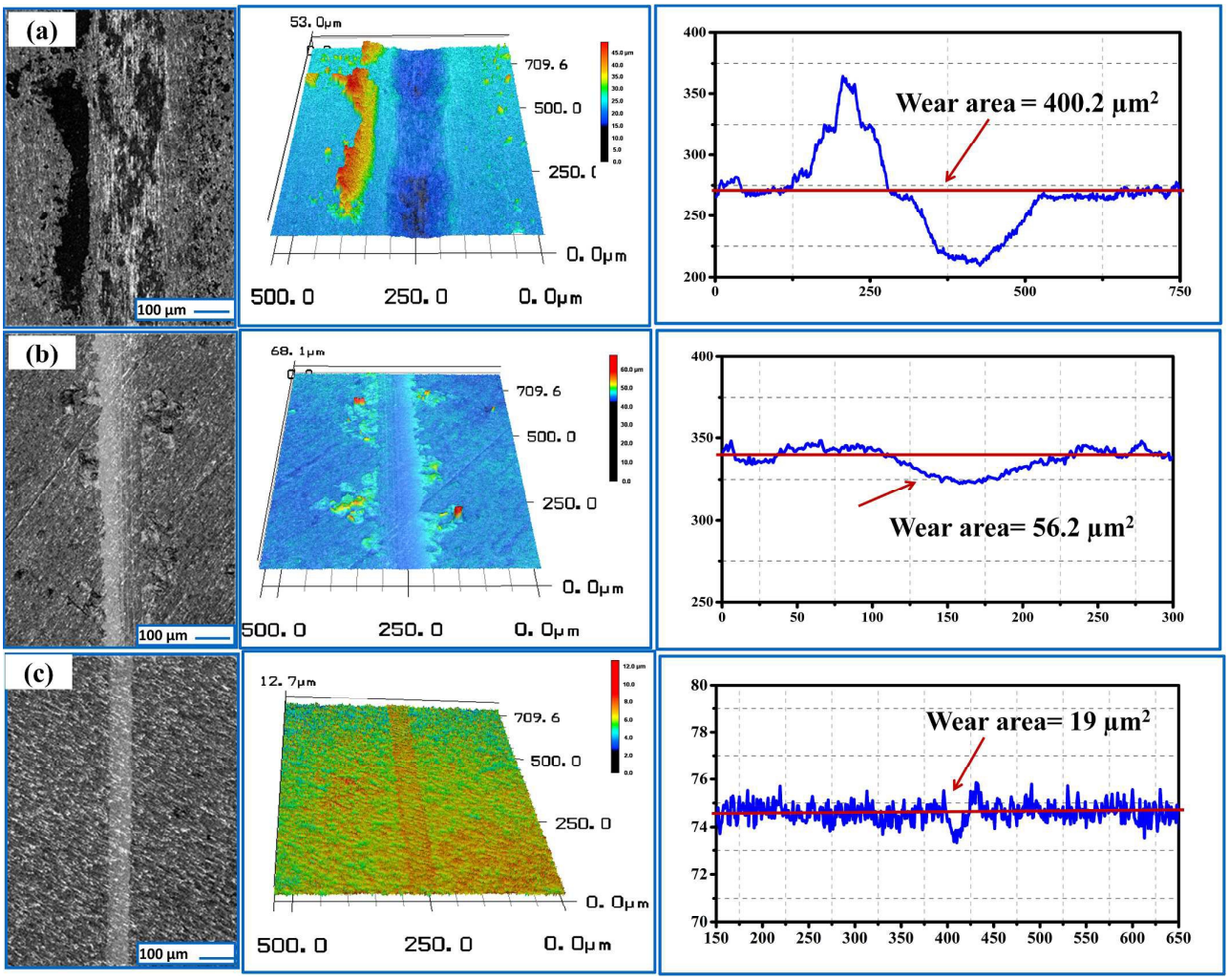

Fig. 6 Laser microscope image, 3D image, and 2D profile of the wear track formed on the specimen surface after 10,000 cycles of sliding under 50 mN normal load and ambient temperature for (a) bare SS, (b) PTFE coated SS, and (c) PG (PTFE+15 vol.% GO) coated SS specimens.

Journal Name

ARTICLE

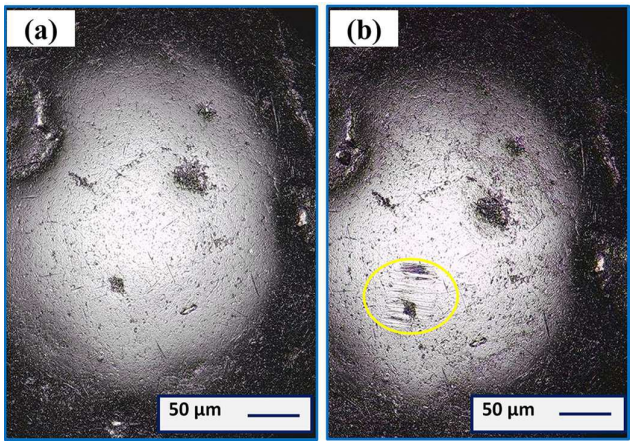

Fig. 7 Laser microscope image of 1 mm SS ball (a) before and (b) after 10,000 cycles of sliding against PG (PTFE+15 vol.% GO) coated SS specimen under 50 mN normal load and ambient temperature. The ellipse in (b) indicates the surface damage incurred by the ball during the sliding test.

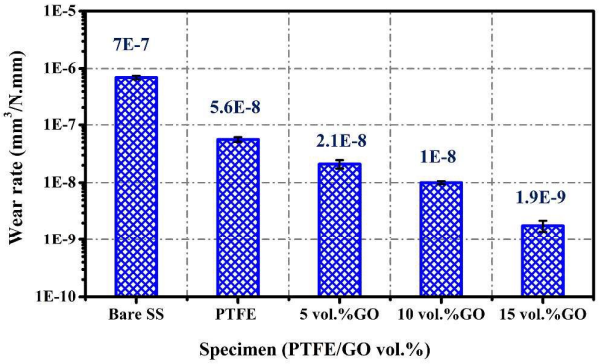

Fig. 8 Wear rate values of bare SS specimen and various coated specimens after 10,000 cycles of sliding under 50 mN normal load and ambient temperature.

Journal Name

ARTICLE

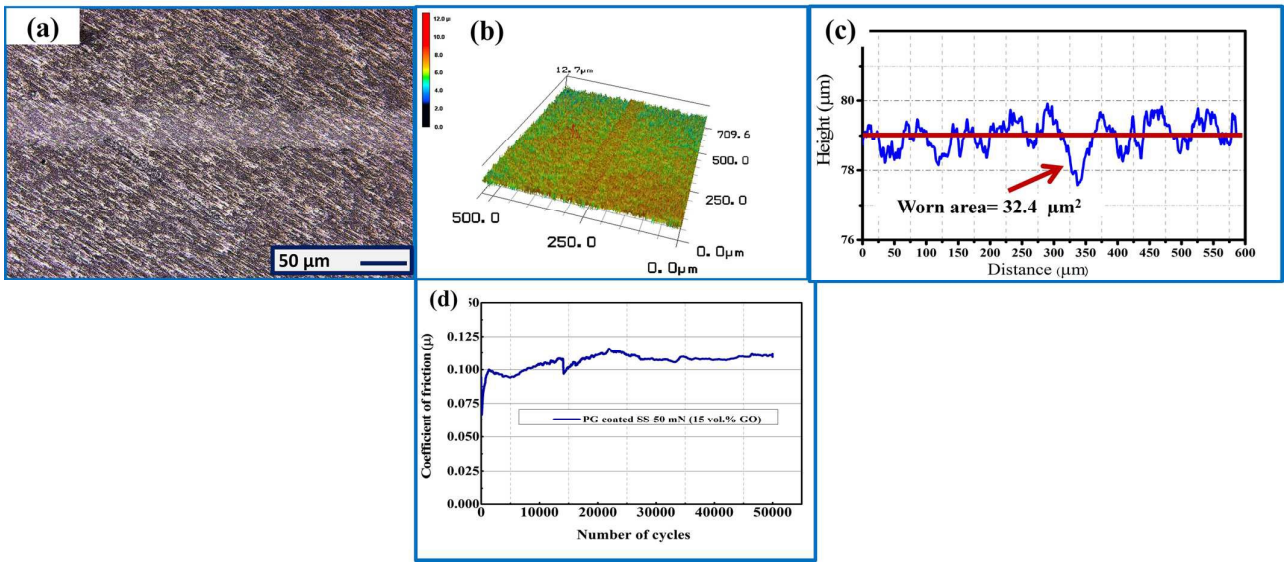

Fig. 9 (a) Laser microscope image, (b) 3D image, (c) 2D profile of the wear track and (d) coefficient of friction with respect to number of sliding cycles for the PG (PTFE+15 vol.% GO) coated SS specimen. Durability test condition was 50,000 cycles of sliding under 50 mN normal load and ambient temperature.

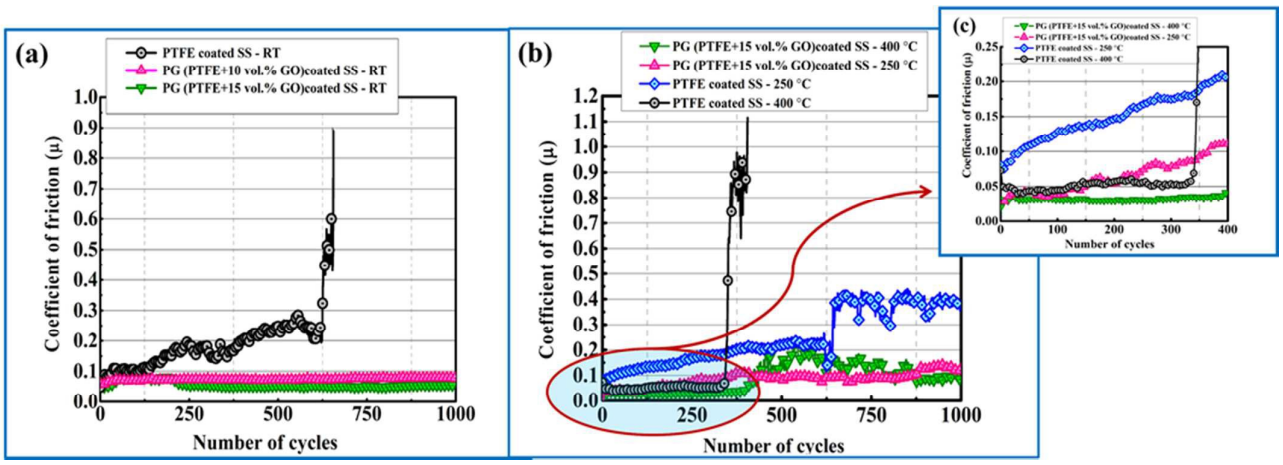

Fig. 10 Coefficient of friction for various specimens with respect to number of sliding cycles under 5 N normal load at (a) ambient temperature, (b) elevated temperatures and (c) magnified inset for better resolution of first 400 cycles of elevated temperature COF data.

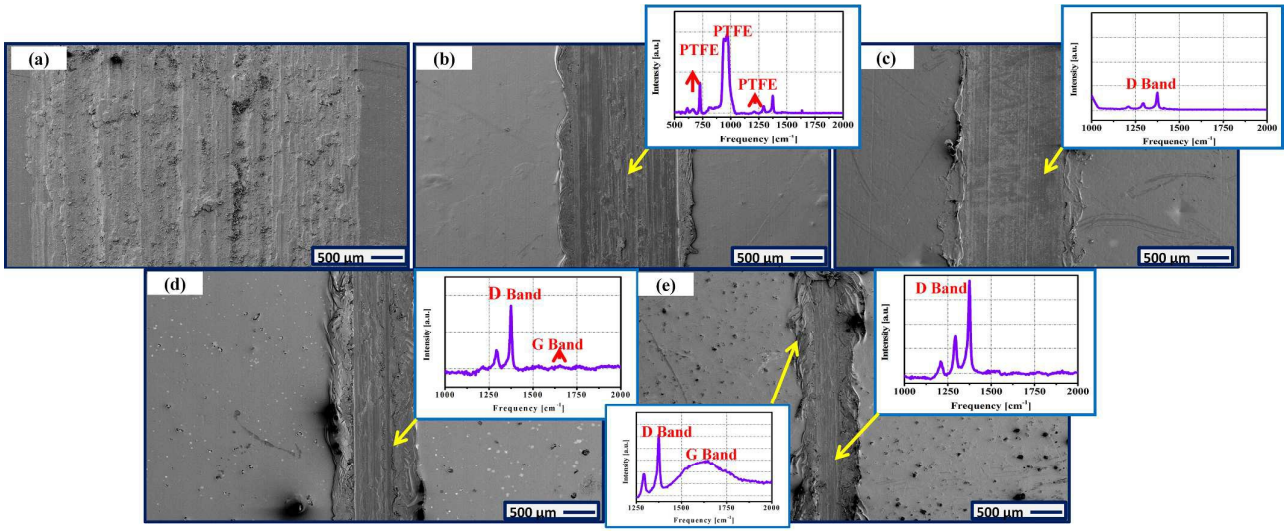

Fig. 11 SEM images and Raman analyses of the wear tracks after 1000 sliding cycles under 5 N normal load at ambient temperature: (a) Bare SS, (b) PTFE coated SS, (c) PG (PTFE+5 vol.% GO) coated SS, (d) PG (PTFE+10 vol.% GO) coated SS, and (e) PG (PTFE+15 vol.% GO) coated SS.

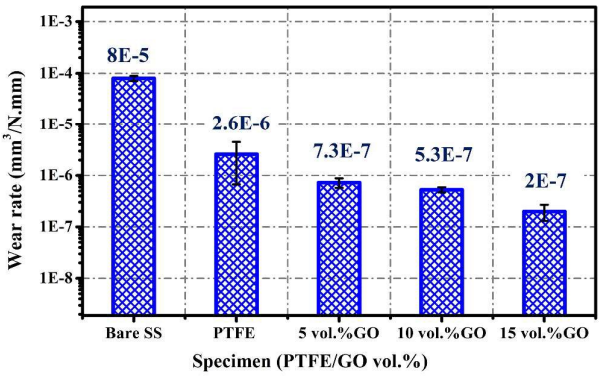

Fig. 12 Wear rate values of bare SS specimen and various coated specimens after 1000 cycles of sliding under 5 N normal load and temperature of 400°C.

Journal Name

ARTICLE

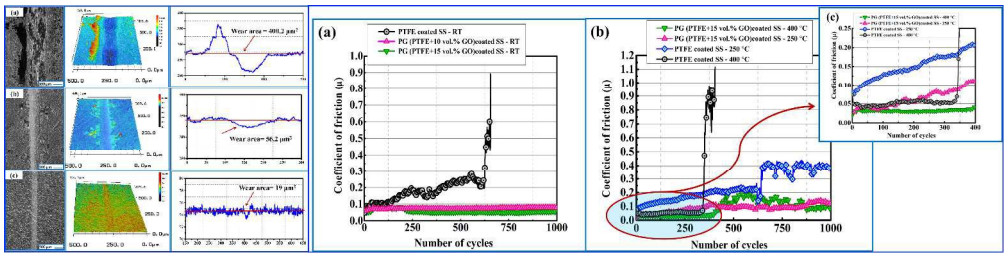

612x151mm (300 x 300 DPI)